

Sedimentological study of the Szőreg-1 reservoir (Algyő Field, Hungary): a combination of traditional and 3D sedimentological approaches



Szilvia Sebők Szilágyi¹ and János Geiger²

¹MOL Plc, Hungary, Exploration & Production; (szsilagyine@mol.hu)

²University of Szeged, Department of Geology and Paleontology, H-6722, Szeged, Egyetem u. 2., Hungary; (matska@geo.u-szeged.hu)

doi: 104154/gc.2012.06

Geologia Croatica

ABSTRACT

The paper presents a 3D sedimentological characterization of a delta plain reservoir. The analysis started with detailed core description studies focusing on the genetic interpretations of the sedimentary structures and multivariate statistical analyses (including Q-mode cluster and R-mode factor analysis), of the sporadic grain-size distributions. These results made the depositional processes of channels, bar-crests and crevasse splays probable. By calibration of the well log responses to the cores with total core recovery, we were able to identify two types of vertical facies transitions: (1) mouth-bars and channels; (2) crevasse splays, crevasse channels and minor mouth bars. In addition, a vertical sequence of a relative thick distributary mouth bar was also recognized. Lateral extension was determined by contouring the sand content on surfaces parallel to the upper time horizon. On these surfaces, the sand content and porosity grid systems facilitated the use of an unconventional 3D geo-cellular modelling approach for both well-log- porosities and sand contents. Since vertical depositional facies were extended into the 3D, rock bodies of the most characteristic channel and mouth bar environments could be cut out from the porosity and sand content models. In this way not only their general geometry and internal characteristics, but also the basic geostatistical features (ratio of anisotropy, the direction of major and minor continuity) of their sand content and porosity were identified.

Keywords: delta environment, 3D model, distributary channel, mouth bar

1. INTRODUCTION

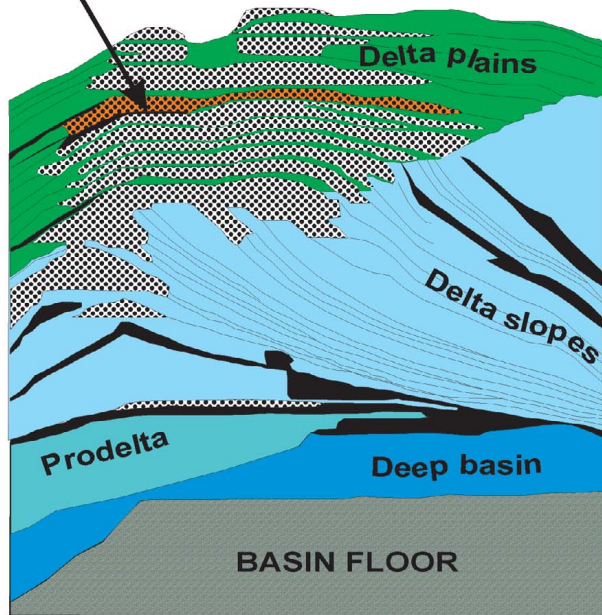
The studied area is located in Central Europe, in the Pannonian basin, South-East Hungary. The **Algyő Field** is the largest Hungarian hydrocarbon accumulation consisting of several oil and gas bearing reservoirs (Fig. 1). A comprehensive description of the structural and geological setting of the field is given in MAGYAR et al. (2006).

The upper members of these reservoirs have developed in a *Pannonian delta system* due to complex lateral shifting and prograding phases. They can be subdivided into *slope* (Algyő Formation) and *delta plain* (Újfalui Formation) rock bodies. The sills of the individual reservoirs were formed

during the delta abandonment phases. Consequently, they can be accepted as *time horizons* in modelling studies. Below these series, the lower reservoirs are regarded as *turbidity rock bodies* (Szolnok Formation) of *partly prodelta fans and partly deep basin origin* (RÉVÉSZ, 1982).

Besides the evident economic importance, the rock bodies comprising the Algyő Field can be considered as an almost complete sequence of general Pannonian (s. l) basin filling accumulation (BÉRCZI & PHILLIPS, 1985; BÉRCZI, 1988). Here, according to the Hungarian Neogene geochronological terminology we use ‘Pannonian (s. l)’ for Late Miocene-, Pliocene sequences. In the Algyő Field, the Pannon-

Szőreg-1 reservoir



ALGYŐ FIELD

Reservoir
Regional sil



Figure 1: Theoretical cross section of the Algyő Field.

ian delta progradation is one of the youngest within the Great Hungarian Plain. On the basis of seismic data, VAKARCS et al. (1994) then VAKARCS (1997) published the first results of mapping the shelf-margins of the prograding basin

filling delta-systems. The most recent results have shown that self-margins reached the vicinity of the Algyő Filed about 5.7 million years ago (MAGYAR, 2010, Fig. 31).

The Szőreg-1 oil reservoir with a large gas cap is one of the largest sedimentary successions within the delta plain record (Fig. 1). Its average gross thickness is about 35 m, but locally it can reach 50 m. Earlier work by RÉVÉSZ (1982) and GEIGER et al. (1998) proved its *delta plain origin* with a significant amount of fluvial channel sedimentation.

The main purposes of this study are to (1) provide a high resolution spatial-temporal description of the sedimentological evolution of the Szőreg-1 reservoir rock body and (2) reveal the real (not simulated) 3D geometry of some depositional subenvironments characteristic of the delta-plain, using 3D contouring of quantitative well-log properties.

Basic aspects of the *geo-cellular 3D modelling*, methods of *well-log calibration*, *multivariable classifications* and *interpretations of the grain size data* have already been published (e.g. PARK, 1974; JORESKOG, 1976; GEIGER, 1986; GEIGER & WEROWSKI, 1992, MOLNÁR & GEIGER, 1995, GEIGER & KOMLÓSI, 1995, GEIGER, 2002; 2004). In this study we emphasize those aspects that can play a significant role in the interpretation of new data.

2. ROCK TYPES OF SZŐREG-1

According to the well logs the internal heterogeneity of Szőreg-1 is considerable (Fig. 2).

On the basis of sporadic cores, the following general picture can be compiled concerning the sedimentary rocks of the reservoir. The general succession starts with *argillaceous marls*, which can alternate with claystone, marl, and coaly argillaceous marl. Their average effective porosity is about 0.07 (7%). Argillaceous marls are also observed at higher stratigraphic positions, too, where they are interbed-

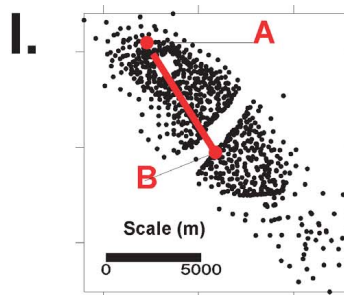
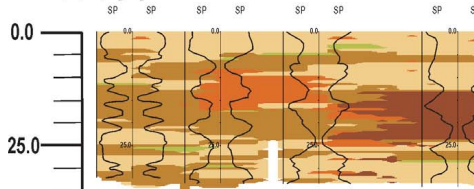


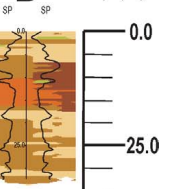
Figure 2: Geological cross section resulting from the 3D lithological model of the Szőreg-1 reservoir.

II.

Depth below the top (m) A



Depth below the top (m) B



Sandstones with carbonate cement
 Medium quality sandstones
 Good quality sandstones
 Poor quality sandstones
 Very poor quality sandstones

ded with *lignite bands*. In this latter situation, the vertical sequence of argillaceous marl, marl and lignite transitions are very characteristic. The thickness of the lignite bands or layers can vary from a few centimetres to tens of centimetres. Foliation and shiny sliding surfaces are important features.

This lower succession expresses *abandonment processes* of the previous delta lobes, as derived from the general sedimentological evolution of the Algyő Field (RÉVÉSZ, 1982, GEIGER 2002, 2004).

Fine siltstones are grey – dark grey rocks showing foliation or earthy cracking. Their average effective porosity is about 0.1 (10%). They contain a great amount of macrofauna, in some places even resembling lumashell too. This rock type is generally rich in *coalified plant fragments*. Fine siltstones show gradual coarsening upward (CU) transition toward coarse siltstones, but they can also be interbedded with thin fine sandstones.

Coarse siltstones are grey with frequently ochre discoloration. Their average effective porosity is about 0.22 (22%). They contain quite high amounts of mica and fine sand. In general, coarse siltstones are laminated, picked out with coalified plant fragments.

Fine sandstones are light grey, and similarly laminated to the coarse siltstones by coalified plant fragments and mica. They usually represent *gradual transitional stages between* coarse sandstones and coarse siltstones. The average effective porosity is about 0.28 (28%).

A yellowish gray colour characterizes coarse sandstones. They can also be *laminated*, but a massive, *structureless development* is also common. In some places, the clay mineral content of the pore space can be high, due to the presence of *syngenetic clay and carbonate minerals*. Carbonate also occurs as carbonate grains. *Horizontal bedding*, and *high and low angle cross bedding/laminations* are the most characteristic sedimentary structures. The average porosity is 0.30–0.32 (30–32%).

Rock types, with the exception of the underlying argillaceous marl, do not form laterally continuous layers. They can be followed to only for tens or hundreds of metres. Interfingering of the different rock types is a typical characteristic almost everywhere within the studied section (Fig. 2).

3. METHODS

A *full-scale relational, sedimentological data base* has been developed which includes qualitative and quantitative data about core analyses, horizontal layering, facies identification, and well log interpretation. For macro sedimentological analysis it contains 382 grain size analyses from 53 wells, 291 routine petrophysical analyses from 356 wells, and 156 Hg-capillarity measurements in 126 wells. Geophysical logs and their quantitative petrophysical interpretations (at 0.2 m intervals) are available from 512 wells penetrating the whole reservoir thickness. They were used for mega-scale sedimentological analysis including study of well-log responses, and 3D modelling.

3.1. Detailed core descriptions and facies identifications

The focus was on genetic interpretations of the *sedimentary structures* and textures, in order to outline both the main depositional processes and the sedimentary facies together with some vertical core profiles. Core descriptions played a significant role in the identification of depositional facies in three key-wells. Descriptions are based on the system suggested by MIALL (1966, 1999). In identification of depositional facies of the delta plain, and delta front succession, publications by REINECK & SINGH (1973), GALLOWAY (1975), WRIGHT (1977), POSTAMA (1995) were useful, together with some recently published Pliocene, Pleistocene and Holocene examples (e.g. HOOGENDOORN et al., 2005, LONGHITANO, 2008; ROHAIN et al., 2008, HOOGENDOORN et al., 2008)

3.2. Multivariate statistical analyses (including Q-mode cluster and R-mode factor analysis) of the sporadic grain-size distributions

According to some earlier works, the lateral variability of the transporting-depositing media can be taken into account by lateral extension of genetic groups determined via *cluster analysis* of grain-size distributions (PARK, 1974; GEIGER, 1986; GEIGER & WEROWSKI, 1992).

For this purpose 382 grain-size distributions have been classified using an r-hierarchical, Q-type clustering technique. In this analysis the *similarity coefficient* was the cosine of the angle between any two vectors representing the samples. The method for reduction was the *centroid* approach (MOLNÁR & GEIGER, 1995).

Sedimentological interpretation of the resulting discrete groups and subgroups was carried out by the combined use of *R-mode factor analysis* (JORESOG, 1976), and interpretation of the identified sedimentary structures. The R-mode factor analysis was applied in a cluster-by-cluster manner to the grain size constituents, with the Md and C value of samples belonging to a particular cluster (JORESOG, 1976, MOLNÁR & GEIGER, 1995).

3.3. Calibration of well log responses to cores with total core recovery

In this phase we used the method introduced in Hungary by RÉVÉSZ (1980), where *Microlog*, *SP* and *Gamma logs* were used for calibration. The resulting “*electrolithological units*” were the tools used to extrapolate the rock types to the uncored regions. Beside this feature, a semi-quantitative measure, the so-called *sand-content* (of 1m thick units), was derived from the types of electrolithologies (Fig. 3, RÉVÉSZ, 1980). This is the sandstone content (in percent) of the rock body with unit cross-sectional area and 1m thick (Fig. 3).

For instance, 80% sand content means that the 80% of the total rock volume can be expected to be sandstone, but it is not necessarily a continuous sandstone layer. This parameter can reflect both the existence and the intensity of the palaeocurrents (RÉVÉSZ, 1980).









IDEALIZED SERIES	MICROLOG SHAPE	NAME OF THE ELECTROLITHOLOGY	NET SAND RATIO
		GOOD QUALITY SANDSTONE	90%
		MEDIUM QUALITY SANDSTONE	75%
		POOR QUALITY SANDSTONE	60%
		ALTERNATION OF SANDSTONE AND SILTSTONE	50%

Figure 3: Electrolithological types and their sand contents defined by micrologs and cores with total core recovery (after RÉVÉSZ, 1980).

3.4. 3D modelling approach and high resolution facies analysis

The huge number of wells penetrating the reservoir facilitated the application of a *special geo-cellular 3D modelling approach* (GEIGER, 2002). Quantitative geophysical interpretations were available at 0.2 m intervals in each well. Applying any vertical interpolation in building 3D models would have smoothed out the small scale vertical variances which are needed for analysis by high resolution stratigraphy. The main goal was to emphasize the stratiform characteristics of the depositional systems within the reservoir

thickness. The easiest method is to (1) cut the reservoir rock body by surfaces parallel with the bottom of the sill; (2) perform lateral parameter estimations on these surfaces; (3) build a 3D model by putting the grid systems of the second step below each other (Fig. 4). If there is no considerable lateral erosion between the top and the bottom of the reservoir, these grid systems should honour the temporal evolution (HOULDING, 1994).

On each cutting surface, the data locations can be identified by crossing the well trajectories and the cutting surfaces. Between any two cutting surfaces, the petrophysical data (coming from well-log interpretations), of the 0.5 m thick vertical intervals were given by the average of the datum falling to these intervals. These average values were assigned to data locations on the cutting surfaces. The algorithm of lateral extension of porosity and sand content readings was the *ordinary kriging with linear semi-variogram model*.

The resulting grid systems can be used in two different ways. On each cutting surface, the grid systems are of the same size. The easting and northing coordinates of each grid node are known. The distance of each nodal point from the topmost surface is also known. This distance is uniformly 0 m on the first cutting surface, 0.5 m on the second one, etc. Note, that in this way we applied the so called *stratigraphical coordinate system* introduced by DEUTSCH (2002). In addition, certain petrophysical values (from the lateral extensions) are also assigned to each grid node. So, there is everything at hand to visualize a geo-cellular 3D model of the rock body (HOULDING, 1994). This is a trivial application of the grid systems.

The grids defined in a vertical sequence, however, can play a significant role in the *high resolution facies analysis* of the key wells, as well. In these wells the depositional facies of the reservoir section are known. That is, at the crossing of a key well trajectory and a particular cutting surface, the depositional facies is already known from the previous steps. The task is to

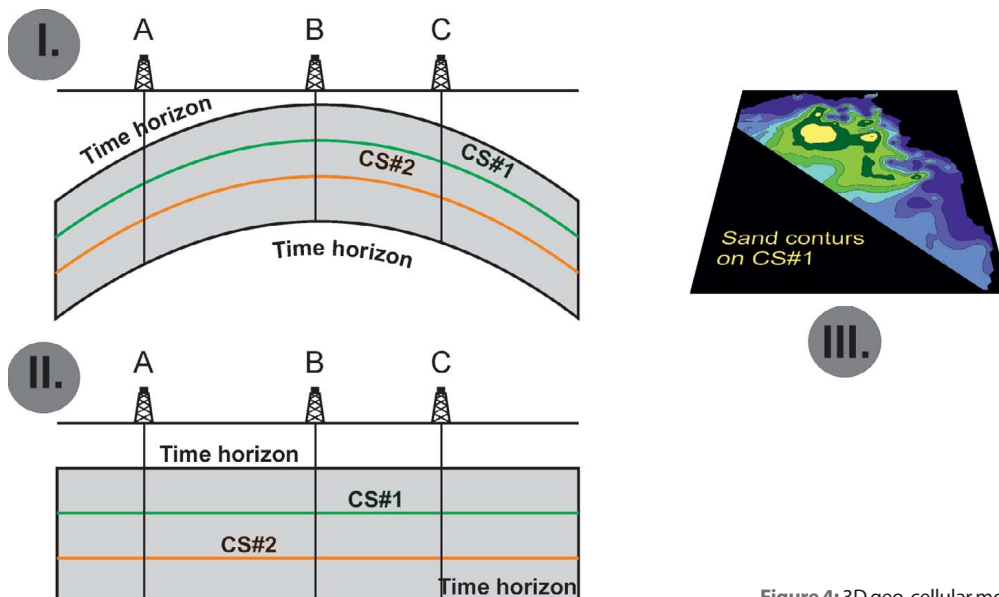


Figure 4: 3D geo-cellular modelling process (after GEIGER, 2002).

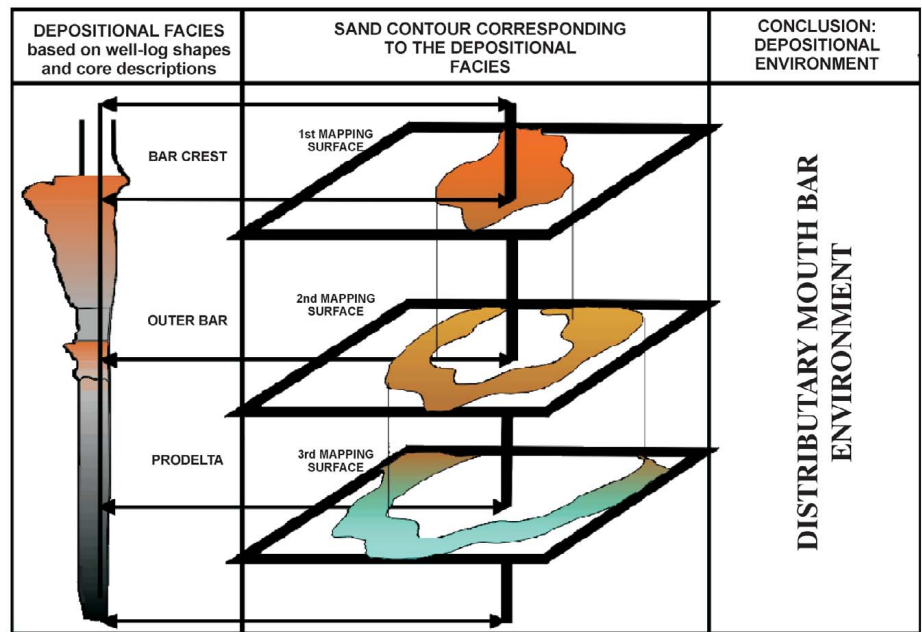


Figure 5: High resolution facies analysis (after GEIGER & KOMLOSI, 1996; GEIGER, 2002).

find that particular sand contour on this surface which coincides with the geometry of the depositional facies identified (Fig. 5). In this way, after drawing the results of facies analysis on the maps, the boundaries of the different depositional environments can be defined by sand isopachs. This method is called high resolution facies analysis, since it gives the 3D geometry of any depositional environment with 0.5 m of vertical resolution (GEIGER & KOMLOSI, 1996, GEIGER, 2002).

This approach has two constraints. Firstly, the topmost surface of this sectioning process should be a time horizon. Secondly, there must not be any tectonic movements, the effects of which are laterally variable.

The sill of the Szőreg-1 reservoir was formed during a delta abandonment phase. Therefore it can be considered as a time horizon in modelling studies. Moreover, at the time of deposition, the top argillaceous marl can be regarded as a quasi-horizontal surface. The seismic interpretations have proven that within the geological time frame of the Szőreg-1 reservoir there were no lateral tectonic movements. So these stacked maps/grids will reflect the depositional history in the time interval of the accumulation of the Szőreg-1 reservoir.

4. RESULTS

4.1. Sedimentary structures

In both the sandstone and coarse siltstone series, the most frequent bedding form is horizontal planar lamination (Fig. 6, A). In coarse siltstones it represents undisturbed sedimentation following Stokes' law, but in sandstones it can be interpreted as a planar bedding in an upper flow regime. The latter proves the existence of strong sand laden currents. Characteristically, the planar beds of the upper flow regime are associated with trough cross bedding (Fig. 6, B). This feature may express channel progradation, which is a natural phenomenon in the course of delta accumulation both in mouth bar evolution, and crevassing.

Fine siltstone and argillaceous marl series often have small sand lenses which can be derived from temporary sandy accumulation from weak currents within interdistributary bays (Fig. 6, C).

Fine siltstones and argillaceous marls exhibit characteristic bioturbation. Load structures and convolutions in the

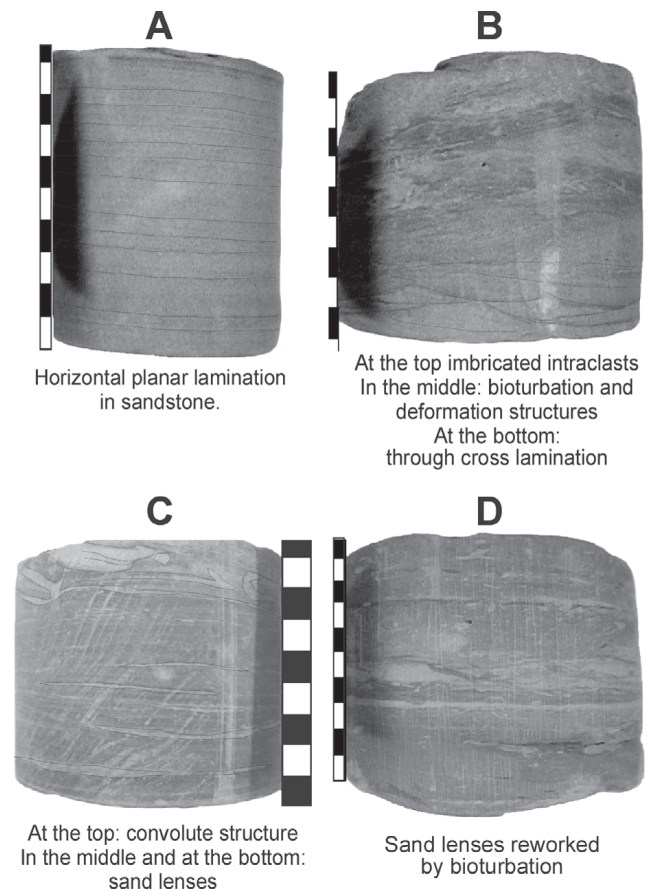


Figure 6: Characteristic sedimentary structures from the Szőreg-1 reservoir.

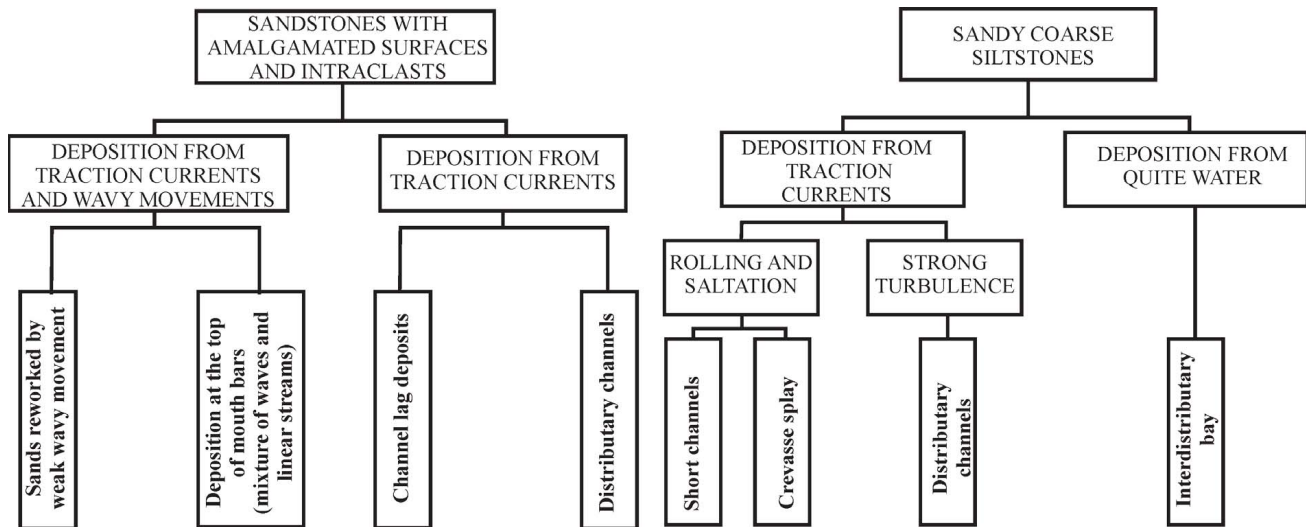


Figure 7: Results of the multivariate analysis of grain size distributions.

form of *soft sediment deformation* are also very frequent (Fig. 6, D).

4.2. Statistical analysis of grain size distributions

The sedimentological interpretations of the discrete groups and subgroups were carried out by combined use of R-mode factor analysis and the interpretation of the identified sedimentary structures. The R-mode factor analysis has been applied in a cluster-by-cluster manner for the grain size constituents, and the Md and C value of grain size distributions.

As a result the samples could be subdivided into *two main groups*. They are *sandy coarse siltstones* and *fine-coarse grained sandstones* (Fig. 7). The sand:silt ratio of samples belonging to the first group is about 1. In this group, beside the *finer parts of active channels*, *interdistributary*

bays and *crevasse splays*, the sediments of *distributary channels* were also identifiable (Fig. 7).

The second group (fine-coarse sandstones) represents the coarse material deposited as *channel-lag* of the active distributaries and the coarser grained sediments of *distributary mouth bars* (Fig. 7).

To study the relationship between grain size distribution and sedimentary facies, the core survey data were genetically divided into five subfacies and 1 transitional subfacies. These include (1) natural levee and channel complexes, (2) distributary channels, (3) crevasse splays, (4) prograding crevasse splays, (5) deposits of swamp and channel abandonments, (6) crevasse and abandonment as a transitional subfacies

Their averaged cumulative grain size distribution curves are shown in Fig. 8.

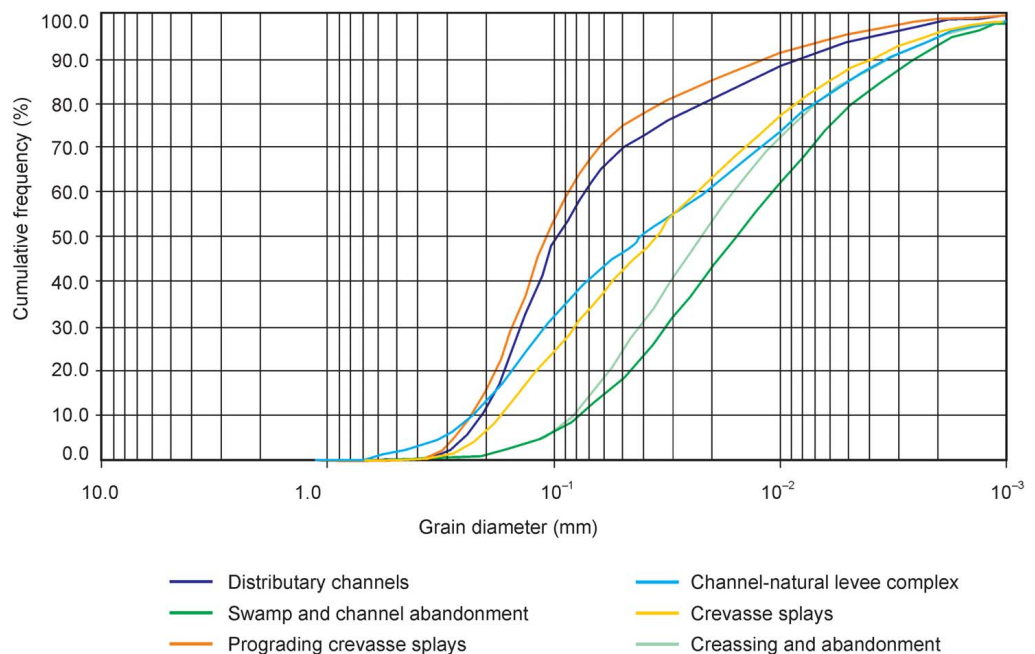


Figure 8: Averaged grain size distributions by depositional facies.

The *swamp-channel abandonments* are the most heterogeneous in the light of grain size distribution. More than 50 % of the sediments are composed of grains smaller than 0.02 mm (fine silt and finer sediments). Sediments with grain-size diameters greater than 0.1 mm are subordinate (Fig. 8).

Crevasse splays are composed of a mixture of grain sizes from two origins. They represent distributary channels, and the remains of natural levees that were occasionally eroded. These sediments were deposited under high transportation energy of flood events. The presence of a coarse grain size and the relatively weak sorting also reflects these processes in the cumulative grain size distribution.

The recurrence of the processes characterized above, can result in the *progradation of crevasse splays*. The outcome of these events is a slightly better sorting texture than that of distributary channels. More, than 50 % of the grains are between 0.1–0.3 mm. This population may have originated from two or three sources: (1) reworked and redeposited material of former crevasse splays, (2) the results of channelization or avulsion, and (3) sediments of natural levees. It has the coarsest grains, which is the result of the higher transporting energy. In contrast, sediments of prograding crevasse splays are the most well sorted, and have the most sloping grain size curves. The frequency of grains smaller than 0.01 mm is around 10 % (Fig. 8).

The average cumulative grain size distribution of the *distributary channels* is similar to that of prograding crevasse splays, but the coarsest grain size is slightly smaller. They are well sorted, with a modal grain-size of fine sand, where 40 % of the grains are between 0.1–0.2 mm (Fig. 8).

The *natural levee – channel complexes* are characterized as a transitional subfacies. The shape of the individual, not averaged, curves can be informative in determining whether it results from an early or late channelizing state of natural levees.

The greatest grain size and the modal grain size class are affected by the greatest and the average energy of sediment transport. Based on the cumulative grain size diagrams of the studied subfacies, the following succession can be established according to decreasing flow velocity: (1) prograding crevasse splays, (2) crevasse channels incised to the deposits of crevasse splays, (3) crevasse splays, (4) natural levee- channel complexes, (5) deposits of late crevasse and abandonment processes, (6) deposits of swamp and channel abandonments (Fig. 8).

4.3. Depositional facies

The identification of depositional facies resulted from hydrodynamic interpretations of sedimentary structures and grain size distributions. Lateral extension of facies away from the vertical columns determined in the wells is demonstrated by the maps of the corresponding mapping surfaces.

4.3.1. Minor mouth bar – channel transition

This transition can be detected in different stratigraphic positions within the reservoir. It can develop when a linear flow

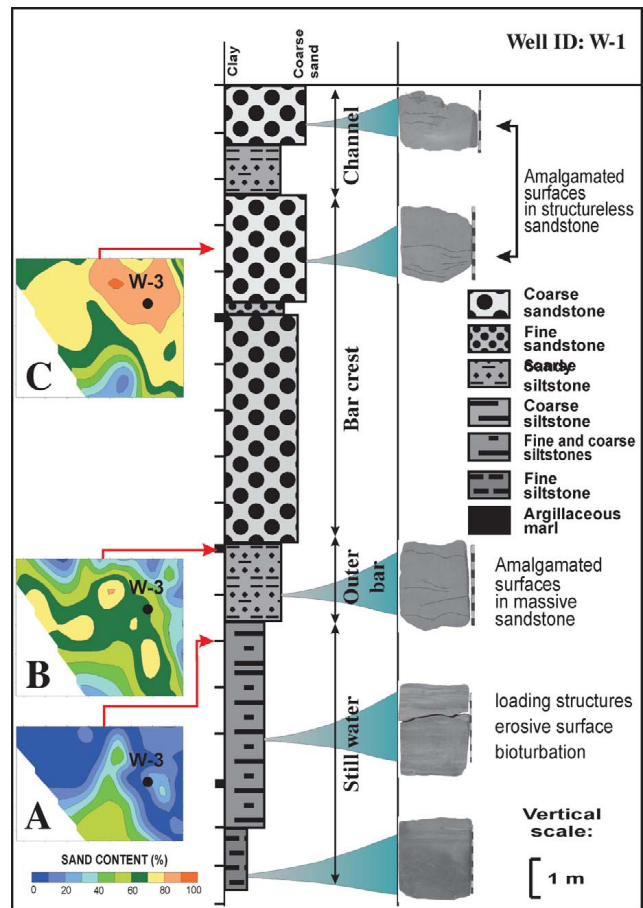


Figure 9: Vertical transition of a mouth bar and channel facies.

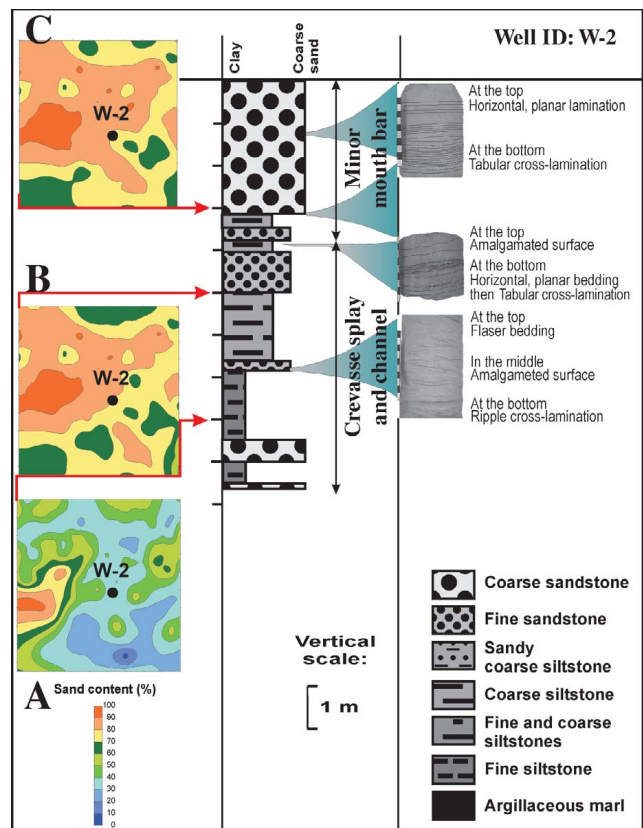


Figure 10: Vertical transitions of a crevasse splay and channel facies.

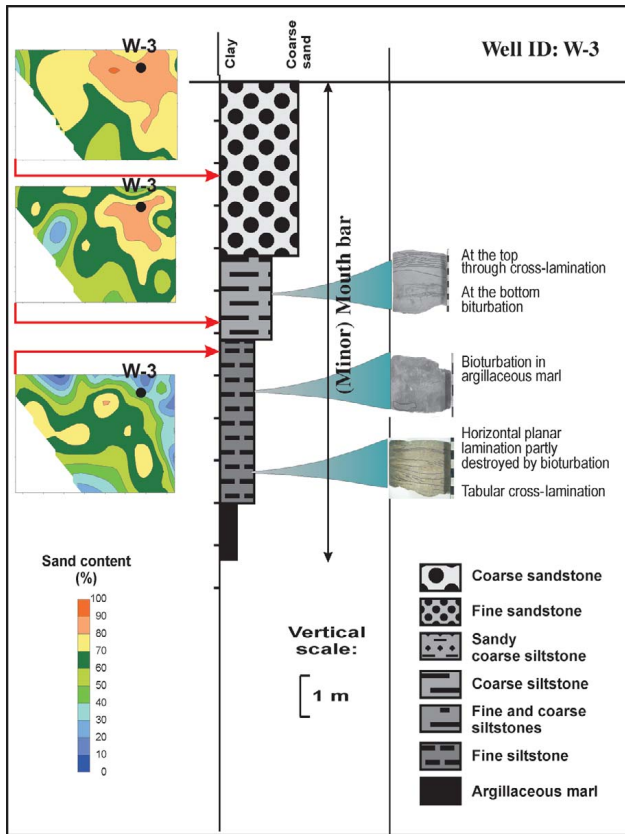


Figure 11: Vertical development of a distributary mouth bar facies.

enters a still water bay. In this situation the sediments of the prograding flow are initially coarse siltstones (Fig. 9, A) which are followed by gradually coarsening sandstones (Fig. 9, B).

On Figs. 9A & B, the still water sedimentation, and geometry of the *outer bar* can clearly be identified. Later, in front of the channel head, a *bar-crest* develops as the result of channel and basin interactions. During this process the accumulation progrades toward the basin or bay. On Fig. 9C, this minor mouth bar appears as a characteristic *kidney-shaped geometry*. The mouth-crest with high sand content can also be identified. In the next phase the distributary channel cuts to the body of the minor mouth bar.

4.3.2. Crevasse splay – Crevasse channel – Minor mouth bar transition

One of the typical examples of crevasse splays is shown on Fig. 10A. The upper part of the core may be identified as a vertical section of a mouth bar. The lateral extension of this facies represents a small channel ‘breaking out’ from the minor bar with a NW–SE depositional strike (Fig. 10, C).

4.3.3. Minor mouth bar facies

In some situations the bar facies appears as a ‘stand-alone’ succession, as in Fig. 11. In addition to the prograding sequence, (upward coarsening grain size tendency), the geometry also shows how bar crest development follows outer bar sedimentation.

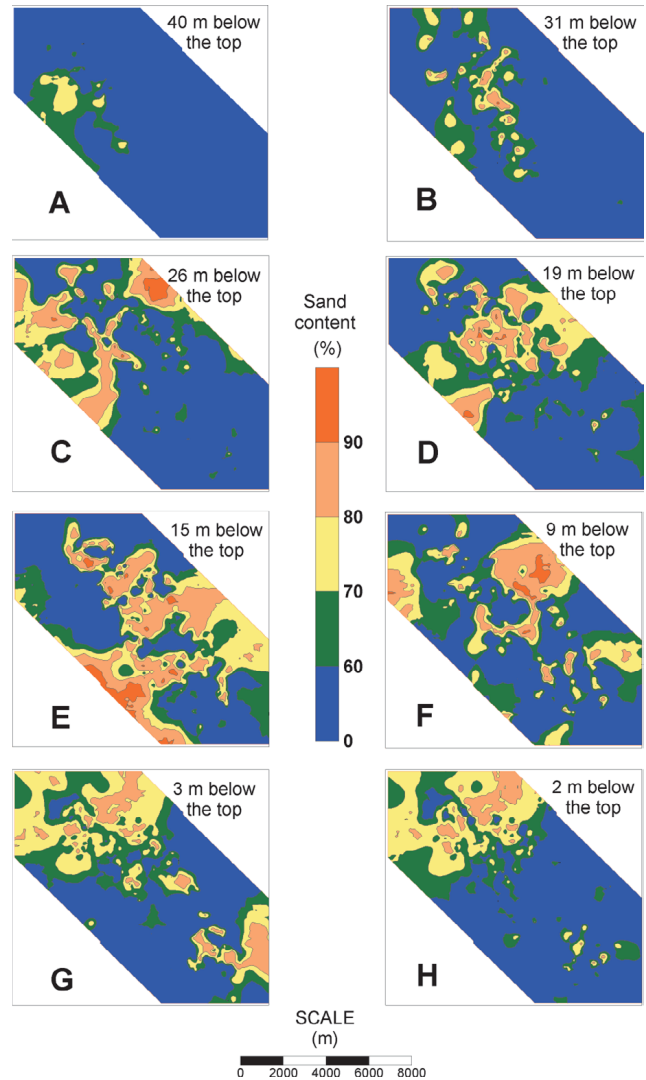


Figure 12: Sand isopach maps on cutting surfaces.

4.4. Sand isopach and facies distribution maps

The modelling process of the rock body was extended to 45 m below the permeable top. This volume was sectioned by surfaces being parallel to the top. The vertical distance between any two surfaces was 0.5 m. Their *lateral resolution* was 100 x 100 metres. The following development can be summarized for the rock body from these maps.

From 40 to 45 m below the top the sedimentological evolution is characterized by quite a large *distributary mouth bar* developed at the south-western rim of the reservoir (Fig. 12, A). The area of this mouth bar is about 14 km², its thickness is about 5 metres. This rock body gradually prograded into a shallow, quiet water bay (Fig. 12, A).

Later the focal point of the bay-filling accumulation shifted to the North–West in the form of a distributary channel. This channel is flanked by *crevasse splays* of different sizes (Fig. 12, B). Its length is about 10–12 km, the average width is 200–300 metres, its thickness is 1–3 metres. This shallow, long channel form is quite characteristic of the recent distributary channels.

Within the interval of 19–29 m below the top, the depositional system is characterized by wider lateral extension of a sandy rock body with > 90% sand content. The equivalent sedimentary rocks are coarse and medium grained sandstones. At that time the focal point of the main depositional processes was in a zone of NE–SW depositional strike (Fig. 12, C & D). The main depositional environments were *bifurcating channels* and small *distributary mouth bars* in front of them (Fig. 12, C and D). The length of the largest bifurcating channel is about 1.5 km, its width is around 200 metres, and the average depth is about 2–3 metres. *Sheet like* sandstone rock bodies were developed by laterally merging (minor) mouth bars. At this time fine siltstone and argillaceous marl sedimentation characterizes the NW and SE regions of the reservoir. Within the central regions, the largest extent of sand can be detected between 10 and 19 m below the top (Fig. 12, E).

From 7 to 10 metres below the top these sandstone bodies are disintegrated (Fig. 12, E) and the main depositional system shifted to the NW part.

Later in this region, a continuous sandy sheet developed while in the SE foreland the accumulation of siltstones, ar-

gillaceous marls and subordinate silty sandstones continued (Fig. 12, G and H). These different identified sandstone bodies represent one hydrodynamic system forming one particular reservoir.

4.5. General characterization of the 3D geometry, porosity and sand content of the significant depositional environments

As outlined above, one of the most important controls on the whole depositional history is a large *distributary channel* with SW–NE depositional strike (Fig. 13 A, B).

This can be studied between 24–27 m below the top of the reservoir. Based on the 3D representation, it reaches a maximum of 5–6 km in length and about 2–400 m width. The average thickness is 2–2.5 m. The 3D form of this channel partly reflects its progradation from the SW to the NE, and partly crevasing from the main channel (Fig. 13 A, B).

The *highest sand content* can be seen along the axis of the channel. The lateral and vertical distributions of its porosity and sand content are *similar* to each other. It is also very characteristic, that the *largest porosity values* belong to the upper part of the channel (Fig. 13, B).

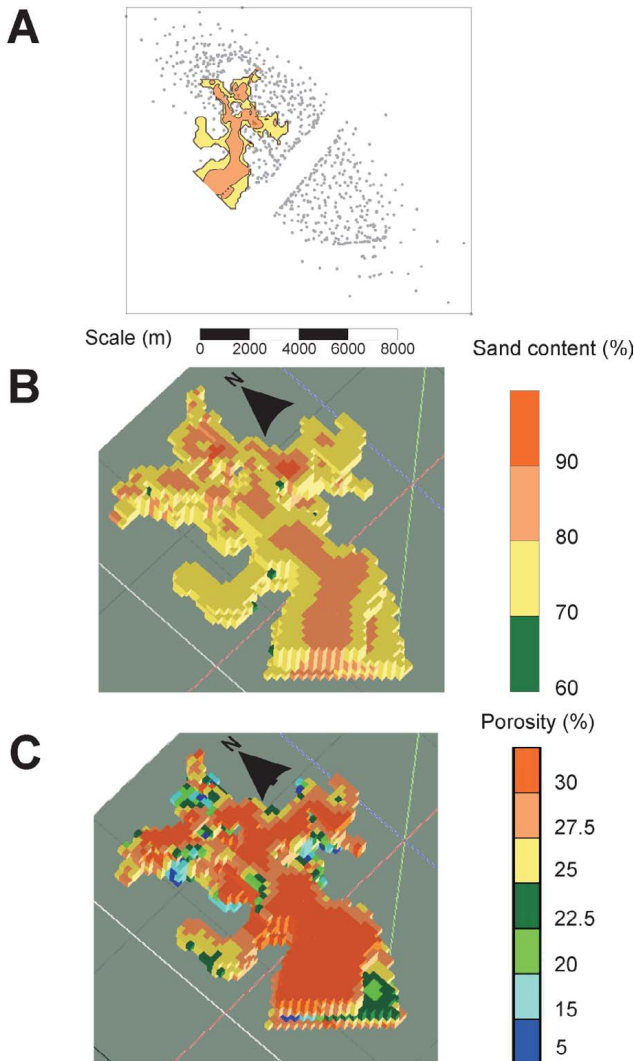


Figure 13: 3D geometry and sand content of a large, bifurcating channel.

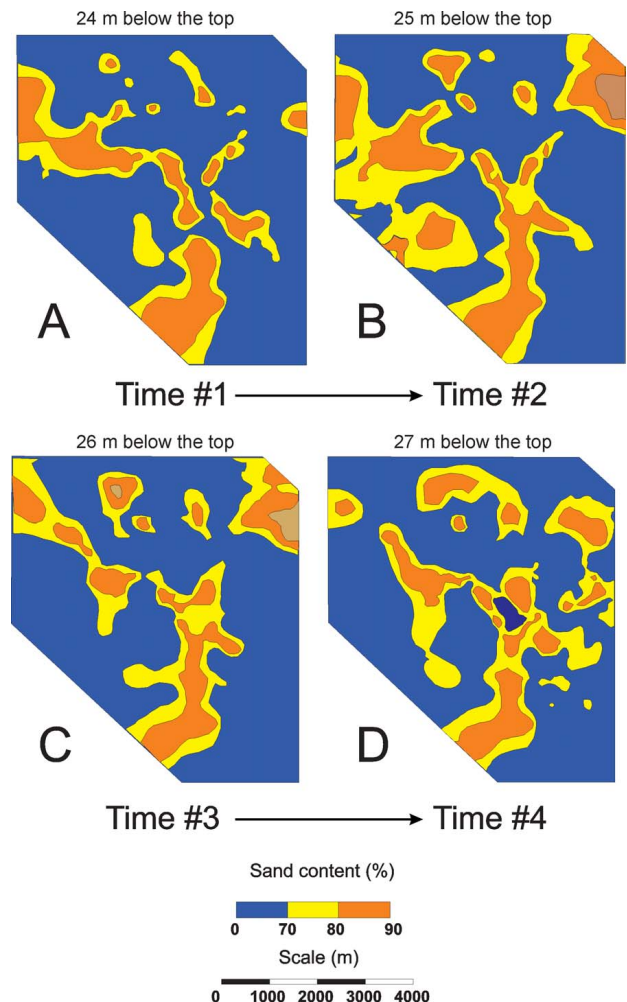


Figure 14: Temporal evolution of a channel system represented in Fig.13

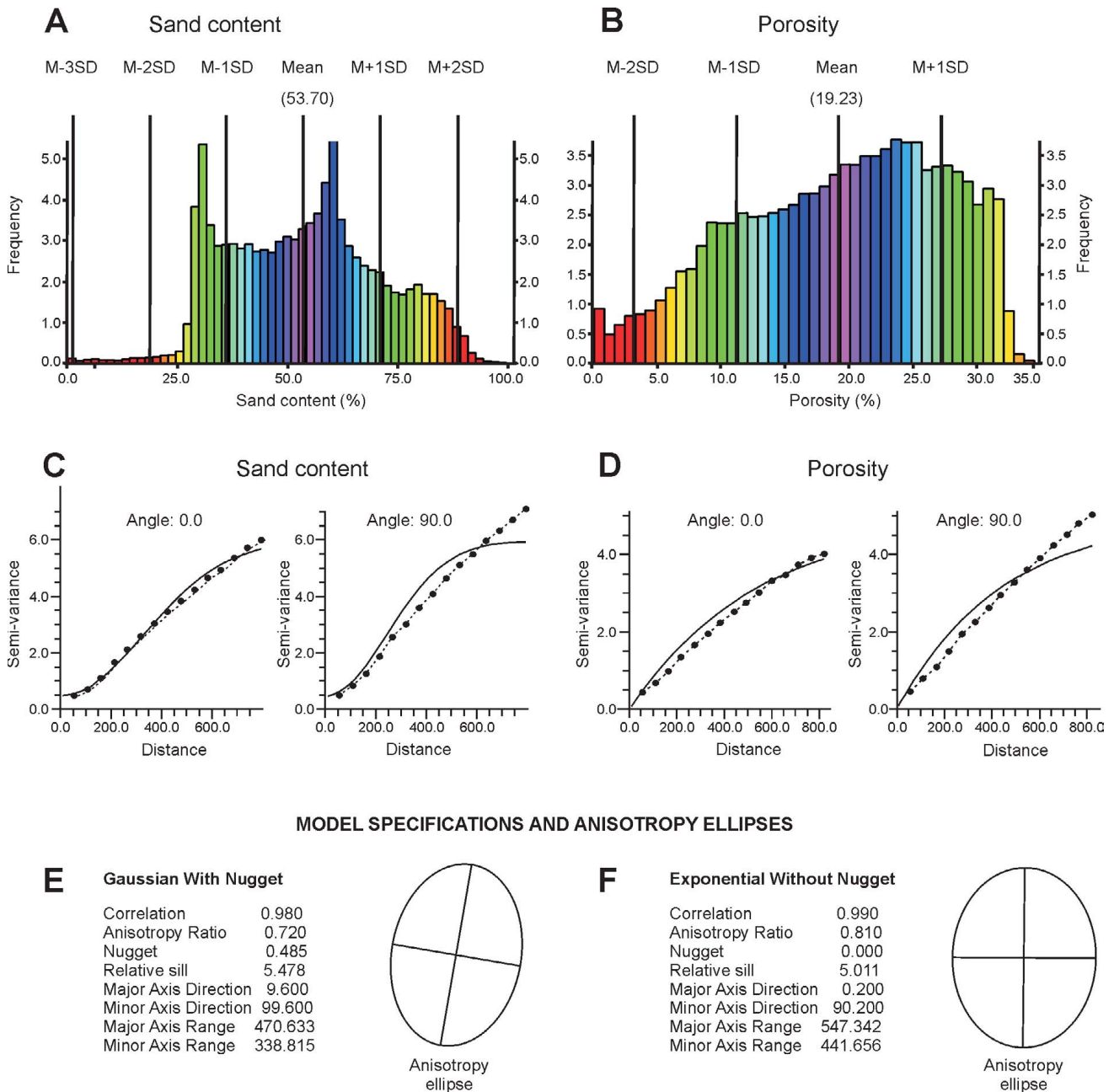


Figure 15: Statistical and geostatistical characters of sand content and porosity grids of the channel shown in Figs.13 and 14. Signs and abbreviations in parts A and B: SD = Standard deviation.

The progradation of this channel system is demonstrated in Fig. 14, A–D.

In addition to the *dendroid channel geometry*, it can also be seen that after a progradation phase, during the still-stand period, a mouth bar type geometry with high sand content developed at the hinterland the channel (Fig. 13, B). It suggests the following *lateral transitions* of the depositional processes: (1) channel progradation, (2) mouth bar evolution, (3) new channel progradation by breaking out from the mouth bar. This sequence is in harmony with the interpretation of both trough cross-bedding and horizontal planar laminations of the core samples coming from a channel environment.

The frequency distributions of the vertically averaged nodal sand content and porosity values in the thickness of

the channel system show *poly-modal* histograms (Fig. 15 A and B) with 80.5 %, and 25.5% averages for sand content and porosity respectively. We have performed *variography analysis* of both average sand content and porosity grids. The results are shown in Fig. 15C and D. The *lateral continuity* of average sand content is quite high, since the Gaussian-type variogram function gave the best model-result. The *main continuity direction* of sand content is comparable to the depositional strike of this rock body (Fig. 14, Fig. 15, E). The *range* in this direction is about 471 m, in the perpendicular direction it is around 339 m. The calculated *ratio of anisotropy* is 0.72 (Fig. 15, E). Since the nugget effect is low, just one-tenth of the sill, this model can characterize almost 90% of the total variance in the terms of linear geostatistics.

In the case of the averaged *porosity* grid, the main continuity direction is much the same as that of the sand content (Fig. 15, E, F). In practice, this suggests that the textural anisotropy may either impact on, or *determine* the spatial variance and continuity of porosity. The similarity of anisotropy ratios (0.72 for sand content and 0.81 for porosity) supports this conclusion (Fig. 15, F).

The next main physiographic units are the *distributary mouth bars*. Among them the larger, south-western one, observable between 34 and 39 m below the reservoir top, significantly affected the initial accumulation phase (Fig. 16, A). Based on the 3D geometric representation (Fig. 16, B, C), its planar area is about 14 km², the thickness is around 5 m. The 3D sand content distribution demonstrates an upward coarsening trend. The *highest sand content* can be seen on its top showing that the background channel cut itself into the bar crest (Fig. 16, B). The spatial distribution of *porosity* does not follow the spatial variation of sand content as close as well as in the case of channel system (Fig. 16, C), although the *upward increasing* effective porosity is typical.

Fig. 17 (A to F) demonstrates its temporal evolution. The characteristic *kidney-shaped geometry* can be clearly recog-

nized on each map. On Fig. 17 (C to F), even the *bar crest* with the highest sand content can also be identified. At the left and right wings of the bar, the development of subaqueous *natural levees* reflects the initial stage of channel cutting and prograding processes (Fig. 17, C). The disturbance of sand contours at the NE border of the bar may represent sliding and slumping deformation being frequent within the distal/outer bar region (Fig. 17, D).

The frequency distributions of vertically averaged sand content and porosity values exhibit good *homogeneity* in the case of sand content and *poly-modality* for the porosity. The average sand content of this bar is 53.7%, the average porosity is 19.23%, though the most characteristic porosity values are around 22.4% (Fig. 18, A, B).

The *lateral continuity* of the sand content is also stronger than that of the porosity (Fig. 18, C, D), since a Gaussian model seemed to be the most appropriate for modelling the semivariance of sand content. In the case of porosity, the semivariogram model was an exponential one. For both properties the *main continuity directions* coincide with the long axis of the bar crest being perpendicular to the direction of bar progradation. The *anisotropy ratios* are the same

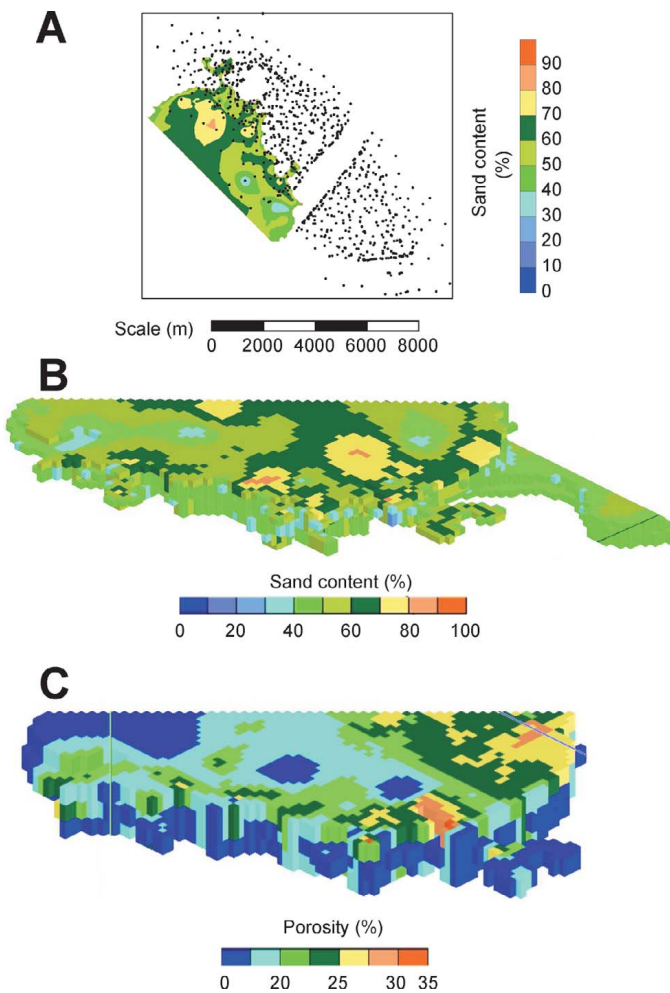


Figure 16: 3D geometry and sand content of a mouth bar. Please note: (1) for better visualization the 'B' and 'C' parts are rotated; (2) although 'A', 'B' and 'C' show the same mouth bar, the 'B' and 'C' parts are rotated.

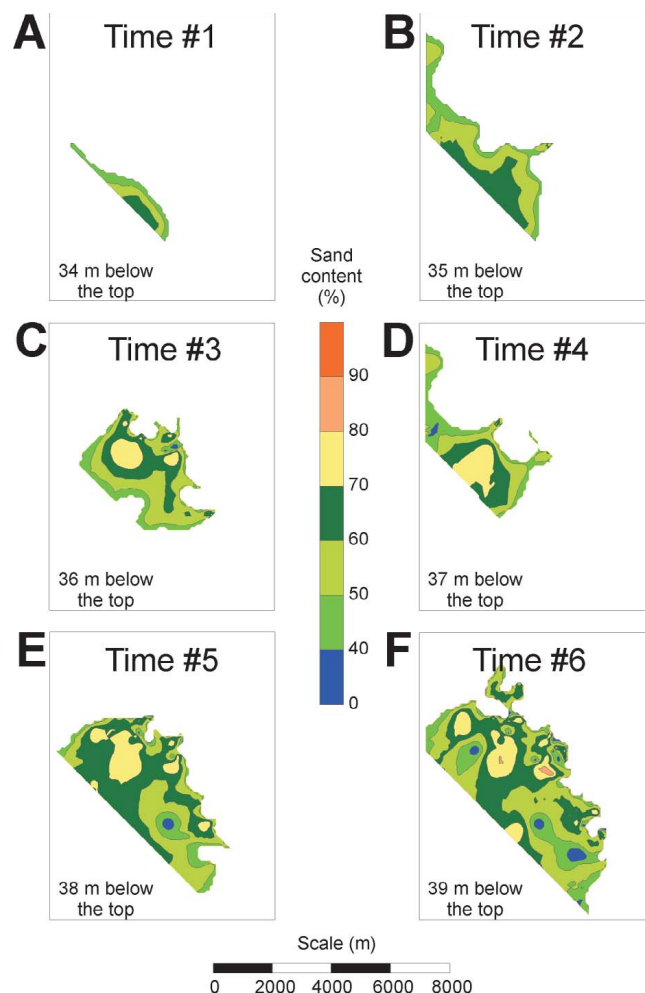


Figure 17: Temporal evolution of a mouth bar represented in Fig.16.

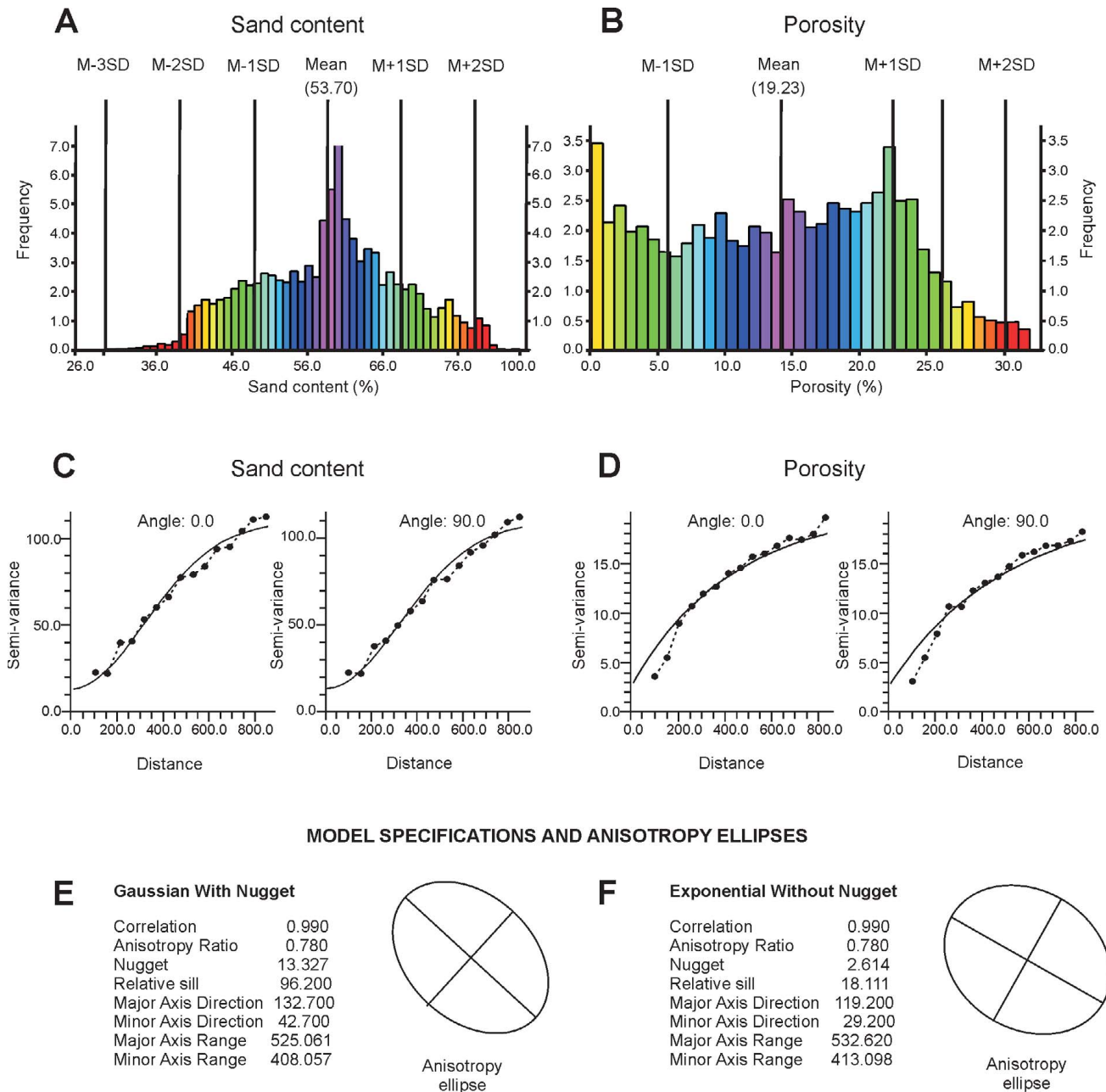


Figure 18: Statistical and geostatistical characters of sand content and porosity grids of the mouth bar shown on Figs.16 and 17. Signs and abbreviations in parts A and B: SD = Standard deviation.

(0.78) for both sand content and porosity, (Fig. 18, E, F). Therefore it suggests that the lateral continuity of textural characters had a significant effect on the spatial characters of effective porosity.

The 3D sand content model of the Szőreg-1 reservoir indicates that a type of sheet sand drape was developed by lateral merging of the “border” mouth bars.

5. DISCUSSION ON THE DEPOSITIONAL HISTORY OF THE SZŐREG-1 RESERVOIR

As a summary, at least *three main depositional processes* should be taken into account in the evaluation of the depositional history based on traditional sedimentological analy-

sis of the core samples, well-log responses, and the 3D modelling of sand and porosity content. They are the followings: (1) development of a mouth bar in the south-western part and a large distributary channel breaking out from this body; (2) development of a mouth bar in the opposite direction; (3) progradation of a large distributary channel from the NW to the SE.

High resolution analysis has revealed that there were *several transport directions from the ‘borders’ to the central parts* in the evolution of this rock body. This analysis also highlighted the *scale* of the most detectable depositional environments. The data and their interpretations have shown that most of the channels were short and several metres in thicknesses. Although the identified mouth bar is relatively

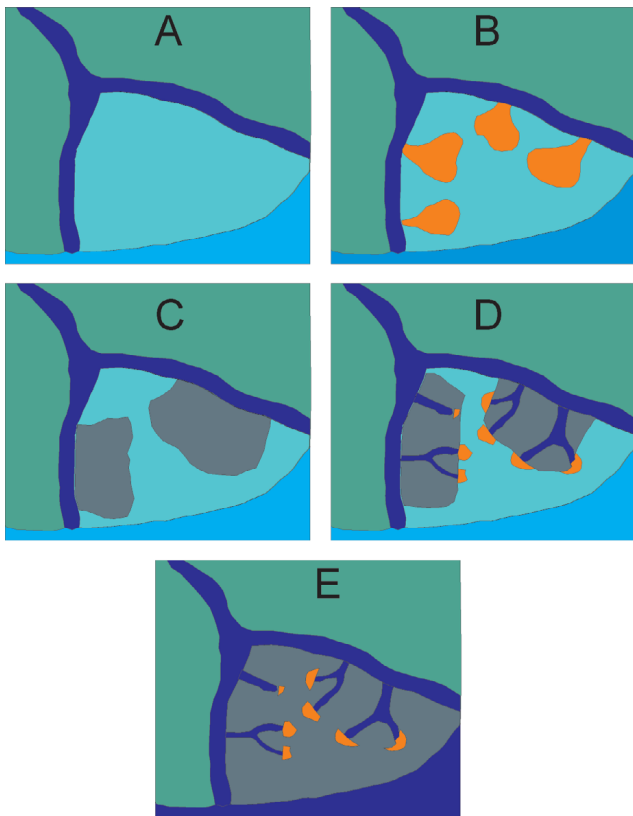


Figure 19: Depositional history of the Szőreg-1 reservoir.

large in its planar area, the recognized thickness is not larger than 5 metres. These scales are not comparable with those of well-developed delta systems which may act in the Pannonian accumulation of the Great Hungarian Plain. The evidence, however, shows a real delta succession. This contradiction can be solved by supposing that this rock body is the result of processes infilling a larger *interdistributary bay*. Some well documented recent examples (e.g. COLOMAN et al., 1964, ELLIOTT, 1978) have shown that in these cases crevassing is the main driving mechanism in the accumulation of interdistributary bays. In this situation, the stabilized crevasse channels with minor mouth bars developed in front of them, can act as delta lobes. The infilling process is achieved by their lateral accretion (ELLIOTT, 1978 p. 107).

According to our results it can be concluded, that quite a large amount of interdistributary bay sedimentation should be taken into account within the study area (Fig. 19, A). During the *initial stage*, the sandy accumulation concentrated in the SW part, where the appearance of one larger and several smaller distributary mouth bars expressed the *preliminary lobe-prograding period* (Fig. 19, B). Later these discrete mouth bar bodies merged and a laterally extended *sheet-like sand body* was formed within the SW region (Fig. 19, C). As a background main channel or delta lobe become more active, new higher energy distributaries *cut down* into this sheet (Fig. 19, D). By their *lateral migration* a new generation of sheet-like sand bodies form and progrades toward the deeper parts of the bay. In front of the channels, new mouth bars develop and merge, meanwhile in the hinterland a typical fluvial deposition dominates (Fig. 19, E).

As a consequence, the above mechanism resulted in the infilling of an interdistributary bay *mimics* larger delta sedimentation. The main difference is obviously the scale and the fact that the driving force, in the accumulation of Szőreg-1, was a multiple source crevassing process and the main delta channels were outside of the study area. According to the depositional strikes they must have been at the SW and NE wing of the Algyő Field.

3D characterization of the revealed channel and minor mouth bar environments also suggests a particular depositional environment where the coincidence of lateral continuity measurements (ratio of anisotropy and the main continuity direction) of sand content and porosity, shows that depositional processes have left a significant fingerprint on the lateral distributions of porosity. It is important to remember that these properties have been determined independently, since the sand content came from qualitative and porosity from quantitative well log interpretations. One of the most trivial interpretations of this result is that the definition of flow units in a dynamic reservoir simulation should rely on the correlation of those steps of sedimentological history which were outlined in Section 4.5.

ACKNOWLEDGEMENT

The authors would like to express their acknowledgement to the Hungarian Oil and Gas Company (MOL Group) for permission to publish these results. Also, many thanks for the two reviewers for their valuable suggestions and comments.

REFERENCES

- BÉRCZI, I. & PHILLIPS, R.L. (1985): Processes and depositional environments within Neogene deltaic-lacustrine sediments, Pannonian Basin, Southeast Hungary.– Eötvös Lóránd Geophysical Institute, Geophysical Transactions, 31/1–3, 55–74.
- BÉRCZI, I. (1988): Preliminary Sedimentological Investigations of a Neogene Depression in the Great Hungarian Plain.– In: ROYDEN, L.H. & HORVÁTH, F. (eds): The Pannonia Basin: a Study in Basin Evolution. AAPG Memoir, 45, 107–116.
- COLEMAN, J.M., CAGLIANO, S.M. & WEBB, J.E. (1964): Minor sedimentary structures in a prograding distributary.– Mar. Geol., 1, 240–258.
- ELLIOTT, T. (1978): Deltas.– In: READING, H.G. (ed): Sedimentary Environments and Facies. Blackwell Scientific Publications, 105–107.
- GALLOWAY, W.E. (1975): Process framework for describing the morphologic and stratigraphic evolution of deltaic depositional systems.– In: BROUSSARD, M.L. (ed.): Deltas, Models of Exploration. Houston Geological Society, 87–98.
- GEIGER, J. (1986): Üledékes homokkötetek szöveti és morfológiai vizsgálata [Textural and morphogenetic study of sedimentary sandstone bodies – in Hungarian].– Földtani Közlemény, 116/3, 249–266.
- GEIGER, J. (2002): A pannóniai Újfalui (Törteli) formációban levő Algyő-delta fejlődéstörténete. I. Az Algyő-delta alkörnyezeteinek 3D modellezése [Depositional history of Algyő-delta (Újfalui (Törteli) Formation: 3D modelling of the subsurfaces of Algyő-delta – in Hungarian].– Földtani Közlemény, 133/1, 91–112.
- GEIGER, J., KISSNÉ, V.K. & KOMLÓSI, J. (1998): A Szőreg-1 telep 3D rezervoár geológiai modellje [3D reservoir geological model of Szőreg-1 reservoir – in Hungarian].– Open-file report of MOL Engineering Office of Research and Development, #156-5636, 216 p.

- GEIGER, J. & KOMLÓSI, J. (1995): 3-D geological simulation of a deltaic reservoir in Hungary.– AAPG Congress, 1995, Nice, Proceedings, 65–80.
- GEIGER, J. & KOMLÓSI, J. (1996): Szedimentológiai, geomatematikai 3-D modellező rendszer törmelék CH-tárolókban [*Sedimentological, geomathematical modelling system in clastic reservoirs – in Hungarian*].– *Kőolaj és Földgáz*, 2, 53–81.
- GEIGER, J. & WEROWSKI, P.V. (1992): Geomathematical modelling of a turbiditic reservoir in SE. Hungary.– In: Amílcar Soares (ed.): *Geostatistics Troia'92*, 1, 311–323, Kluwer Academic Publishers, Dordrecht–Boston–London.
- HOOGENDOORN, R.M., BOELS, J.F., KROONENBERG, S.B., SIMMONS, M.D., ALIYEVA, E., BABAZADEH, A.D., & HUSEYNOV, D. (2005): Development of the Kura delta, Azerbaijan: a record of Holocene Caspian Sea-level changes.– *Mar. Geol.*, 222/223, 359–380. doi:10.1016/j.margeo.2005.06.007
- HOOGENDOORN, R.M., OVEREEM, I. & STORMS, J.E.A. (2008): Process-response modelling of fluvio-deltaic stratigraphy.– *Comput. Geosci.*, 34, 1394–1416. doi:10.1016/j.cageo.2008.02.006
- JORESKOG, K.G. (1975): Geological factor analysis (Methods in Geomathematics, Vol. 1).– Elsevier, 190 p.
- LONGHITANO, S.G. (2008): Sedimentary facies and sequence stratigraphy of coarse-grained Gilbert-type deltas within the Pliocene thrust-top Potenza Basin (Southern Apennines, Italy).– *Sediment. Geol.*, 210, 87–110. doi:10.1016/j.sedgeo.2008.07.004
- MAGYAR, I. (2010): A Pannon medence ösföldrajza és környezeti viszonyai a késő miocénben [*Paleogeographical and paleoenvironmentological characters of the Pannonian basin in the Late Miocene – in Hungarian*].– *GeoLitera*, Szeged, 140 p.
- MAGYAR, I., FOGARASI, A., VAKARCS, G., BUKÓ, L. & TARI, C., G. (2006): The largest hydrocarbon field discovered to date in Hungary: Algyó.– In: GOLONKA, J. & PICHA, F.J. (eds.): *The Carpathians and their foreland: geology and hydrocarbon resources*. AAPG Memoir, 84, 619–632 p.
- MIALL, A.D. (1966): *The geology of fluvial deposits*.– Springer, 582 p.
- MIALL, A.D. (1999): In defense of facies classifications and models.– *J. Sediment. Res.*, 69/1, 2–5.
- MOLNÁR, B. & GEIGER, J. (1995): Possibility for subdividing apparently homogeneous depositional sequences by combined use of sedimentological, paleontological and mathematical methods.– *Geological Journal*, 36, 2/3, 169–177.
- POSTMA, G. (1995): Causes of architectural variations in deltas.– In: OTI, M.N. & POSTMA, G. (eds.): *Geology of Deltas*. Balkema, Rotterdam, 3–16.
- REINECK, H.E. & SINGH, I.B. (1973): *Depositional sedimentary environments*.– Springer Verlag, New York, 103–142.
- RÉVÉSZ, I. (1980): Az Algyó-2 telep földtani felépítése, üledékföldtani heterogenitása és ösföldrajzi viszonyai [*Hydrocarbon deposits Algyó-2: geological structure, sedimentological heterogeneity and paleogeographic features – in Hungarian*].– *Földtani Közlöny*, 110, 512–539.
- ROHAIS, S., ESCHARD, R. & GUILLOCHEAU, F. (2008): Depositional model and stratigraphic architecture of rift climax Gilbert-type fan deltas (Gulf of Corinth, Greece).– *Sediment. Geol.*, 210, 132–145. doi:10.1016/j.sedgeo.2008.08.001
- VAKARCS, G., VAIL, P.R., TARI, G., POGÁCSÁS, GY., MATTICK, R.E., & SZABÓ, A. (1994): Third-order Middle Miocene-Early Pliocene depositional sequences in the prograding delta complex of the Pannonian basin.– *Tectonophysics*, 240, 81–106.
- VAKARCS, G. (1997): *Sequence stratigraphy of the Cenozoic Pannonian basin, Hungary*.– Unpubl. PhD Thesis, Rice University, Houston, Texas, 514 p.
- WRIGHT, L.D. (1977): Sediment transport and deposition at river mouths: a synthesis.– *Geological Society of America Bulletin*, 88, 43–53.

Manuscript received June 26, 2011

Revised manuscript accepted December 12, 2011

Available online February 25, 2012